

Supporting information

Protected Lignin Biorefining through Cyclic Extraction: Gaining Fundamental Insights on Tunable properties of Lignin by Chemometrics

Maria Karlsson^{a,b*}, Vijaya Lakshmi Vegunta^b, Raghu Deshpande^b and Martin Lawoko^{a,b*}

Contents

1. HSQC	2
1.1 Assignment of diagnostic chemical shifts, HSQC	2
1.2 Semi-quantification of inter-unit linkages from the design serie	2
1.3 Semi-quantification of inter-unit linkages, Alcell and kraft.....	3
1.4 Lignin spectra, D1-D15.....	4
1.5 Lignin spectra, Alcell and Kraft	11
1.6 Water fraction from the cyclic organosolv extraction.....	13
1.7 Hemicellulose fraction from the hot water extraction.....	13
2. ³¹ P NMR.....	14
2.1 Assignment of chemical shifts, ³¹ P NMR.....	14
2.2 Assigned phenolic hydroxyl-functionalities.....	14
2.3 Trends of aliphatic and aromatic hydroxyl functionalities	15
3. ¹³ C NMR.....	16
4. Size Exclusion Chromatography (SEC).....	16
5. Differential Scanning Calorimetry (DSC)	17
6. X-ray diffraction (XRD)	17
7. Experimental design.....	18
7.1 Design matrix of the Box-Behnken design.....	18
7.2 Tuning of the models.....	18
7.3 Observed vs. predicted plot.....	19
7.4 Normal probability plots.....	20
7.5 Normalized coefficient plot for Mn and Đ.....	21
7.6 Response surface plots	22
8. Mass balance.....	24
9. Consolidated biorefinery concept.....	26
10. Carbohydrate analysis.....	27
11. Green metrics.....	28

1. HSQC

1.1 Assignment of diagnostic chemical shifts, HSQC

Table S1. Chemical shifts for the quantification of the inter-unit linkages. The C2-aromatic signal was used as an internal standard reference.

Shift	C2	$\beta\text{-O-4}'_\alpha$	$\beta\text{-O-4}'_{\text{Et},\alpha}$	$\beta\text{-O-4}'_\beta$	DBDO $_\beta$	$\beta\text{-5}'_\alpha$	$\beta\text{-}\beta'_\alpha$	$\beta\text{-1}',$ stilbene $_\alpha$	$\beta\text{-5}',$ stilbene $_\beta$	Coumaryl-aldehyde $_\alpha$	Enolether $_\alpha$	HK $_\gamma$
^1H	7.80-6.05	5.41-4.40	4.77-4.13	4.58-4.00	4.01-3.70	5.80-5.16	4.77-4.5	7.10-6.90	7.44-7.167	7.80-7.40	6.27-6.07	4.26-4.09
^{13}C	113.2-102.0	73.8-68.7	81.0-77.3	89.0-80.5	87.8-82.9	91.0-83.2	86.4-83.1	127.8-124.4	121.0-116.9	156.4-151.0	113.7-110.4	68.5-64.6

1.2 Semi-quantification of inter-unit linkages from the design series.

Table S2. Quantification of inter-unit linkages, % per 100 Ar.

Design entry	$\beta\text{-O-4}'_\alpha$	$\beta\text{-O-4}'_{\text{Et},\alpha}$	¹ Sum $\beta\text{-o-4}_\alpha$	DBDO $_\beta$	$\beta\text{-5}'_\alpha$	$\beta\text{-}\beta'_\alpha$	Stilbene, $\beta\text{-1}'_\beta$	Stilbene, $\beta\text{-5}'_\beta$	Coumaryl-aldehyde $_\alpha$	Enolether $_\alpha$	HK $_\gamma$
1	20.1	11.8	31.9	2.79	13.5	1.73	4.90	2.70	1.37	0.730	0.305
2	10.3	10.5	20.8	0.00	9.22	1.64	2.67	3.82	0.99	1.81	0.960
3	18.5	15.7	33.9	2.25	13.9	1.67	4.60	2.88	1.36	0.61	0.390
4	8.43	11.9	20.3	0.00	8.37	1.63	2.83	3.85	0.83	1.65	0.960
5	20.8	9.77	30.5	2.34	13.0	1.61	5.46	2.89	1.49	0.730	0.445
6	15.0	19.2	34.2	1.63	11.9	1.68	3.70	2.27	1.33	1.27	0.755
7	18.7	16.9	35.6	2.41	13.7	1.82	4.46	1.87	1.47	1.07	0.335
8	8.41	11.9	20.4	0.00	7.45	1.42	2.52	2.90	1.13	2.42	1.040
9	17.7	17.1	34.8	2.47	13.6	1.60	4.57	1.81	1.55	1.07	0.485
10	15.5	21.0	36.5	2.39	13.9	1.69	4.16	1.84	1.35	1.10	0.400
11	13.8	16.9	30.7	1.74	12.1	1.51	3.67	2.57	1.22	1.47	0.765
12	12.5	22.3	34.7	1.54	12.1	1.68	3.45	2.29	1.21	1.45	0.615
13-15 ²	15.0 ± 0.480	20.8 ± 0.164	35.8 ± 0.395	1.72 ± 0.081	13.2 ± 0.370	1.66 ± 0.064	3.92 ± 0.057	2.02 ± 0.133	1.36 ± 0.050	1.18 ± 0.030	0.573 ± 0.044

¹The sum refers to the hydroxylated and the etherified alpha position on the $\beta\text{-o-4}'$ inter-unit linkage.

2 n=3 ± SD

1.3 Semi-quantification of inter-unit linkages, Alcell and kraft

Table S3. Quantification of inter-unit linkages, % per 100 Ar.

Sample	$\beta\text{-O-4}'_\alpha$	$\beta\text{-O-4}'_{\text{Et},\alpha}$	¹ Sum $\beta\text{-O-4}_\alpha$	DBDO _β	$\beta\text{-5}'_\alpha$	$\beta\text{-}\beta'_\alpha$	Stilbene, $\beta\text{-1}'_\beta$	Stilbene, $\beta\text{-5}'_\beta$	Coumaryl- aldehyde _α	Enolether _α	HK _γ
Alcell	3.49	3.43	6.92	0.00	2.34	0.49	1.93	2.69	0.41	1.83	0.77
Kraft	6.80	0.00	6.80	0.00	1.66	1.39	2.94	6.17	0	2.59	0.00

¹The sum refers to the hydroxylated and the etherified alpha position on the β-o-4' inter-unit linkage

1.4 Lignin spectra, D1-D15

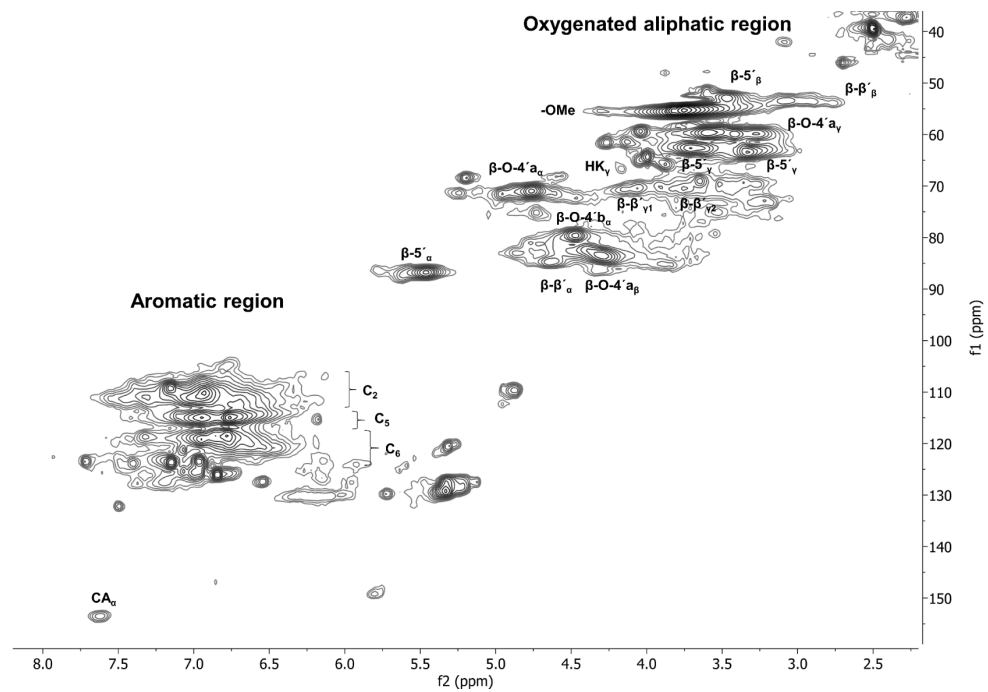


Figure S1. HSQC spectra of lignin sample D1. f1: ^{13}C , f2: ^1H .

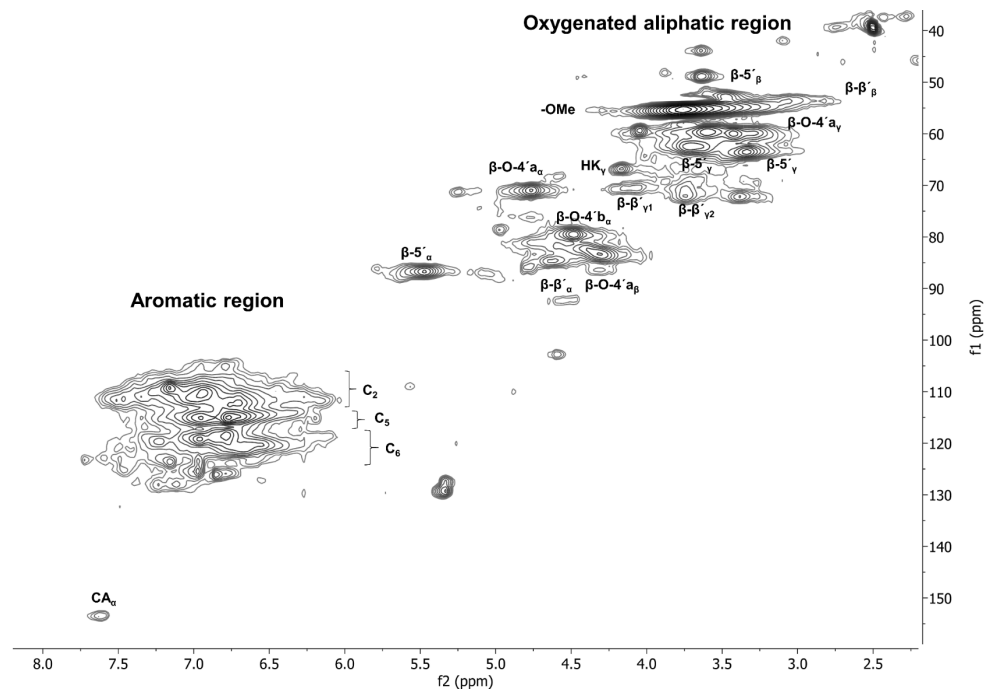


Figure S2. HSQC spectra of lignin sample D2. f1: ^{13}C , f2: ^1H .

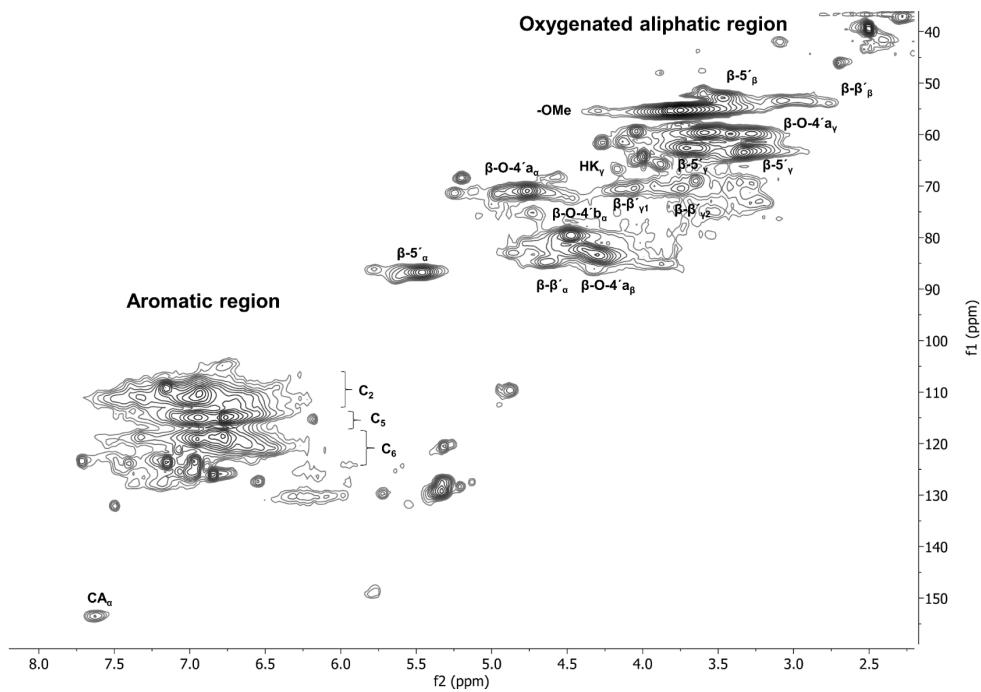


Figure S3. HSQC spectra of lignin sample D3. f1: ^{13}C , f2: ^1H .

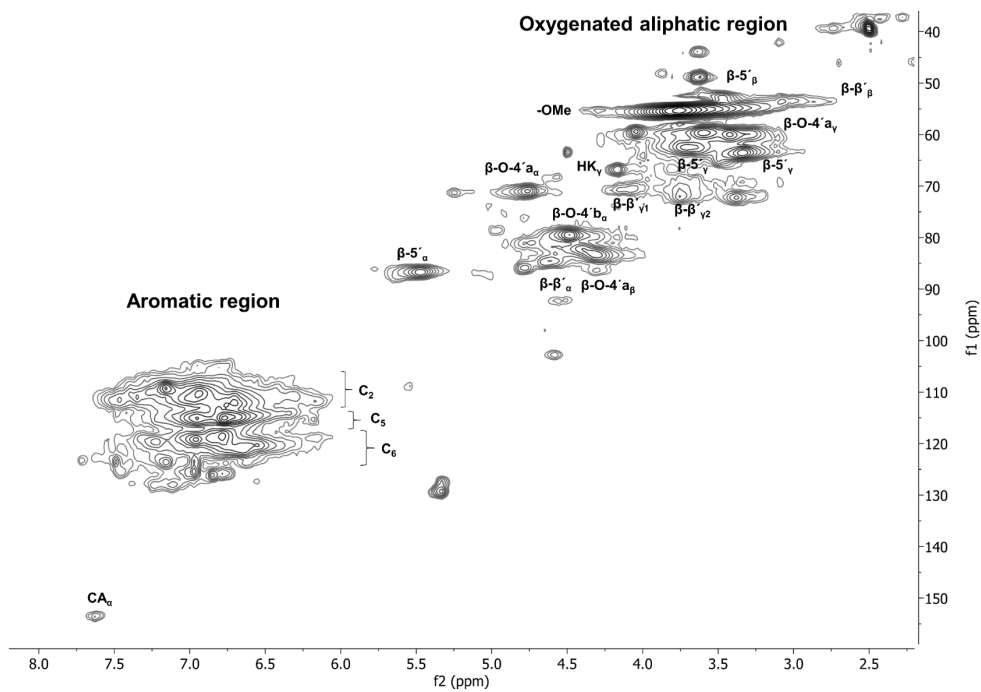


Figure S4. HSQC spectra of lignin sample D4. f1: ^{13}C , f2: ^1H .

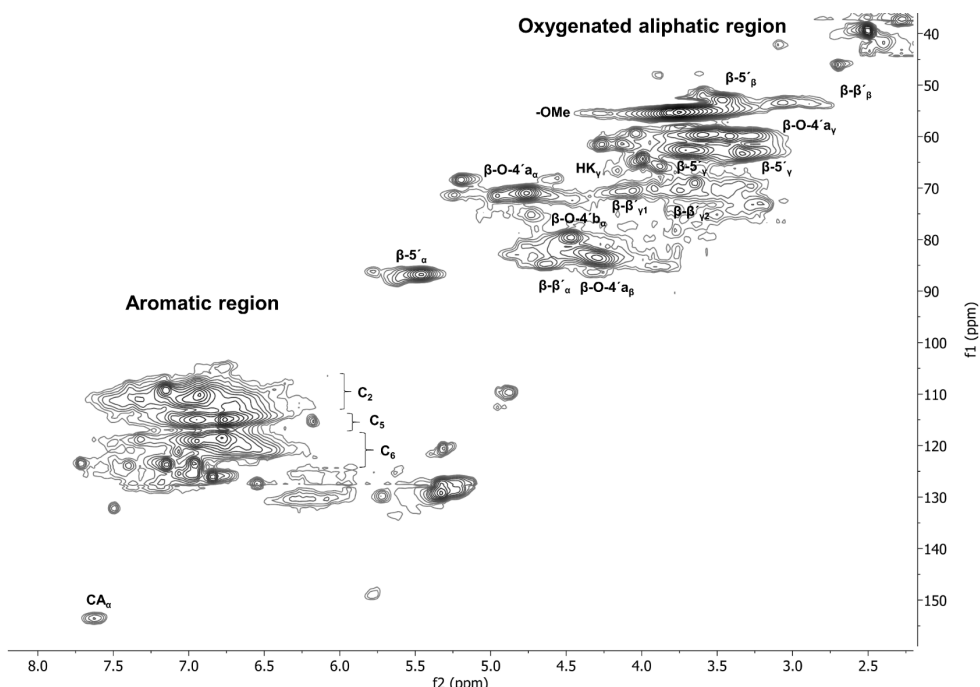


Figure S5. HSQC spectra of lignin sample D5. f1: ^{13}C , f2: ^1H .

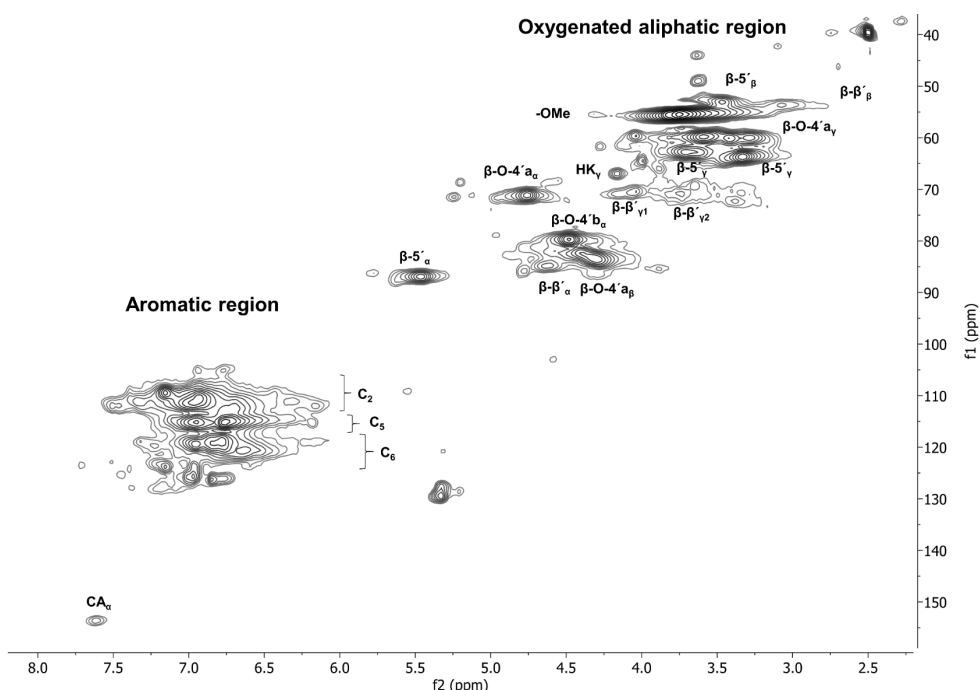


Figure S6. HSQC spectra of lignin sample D6. f1: ^{13}C , f2: ^1H .

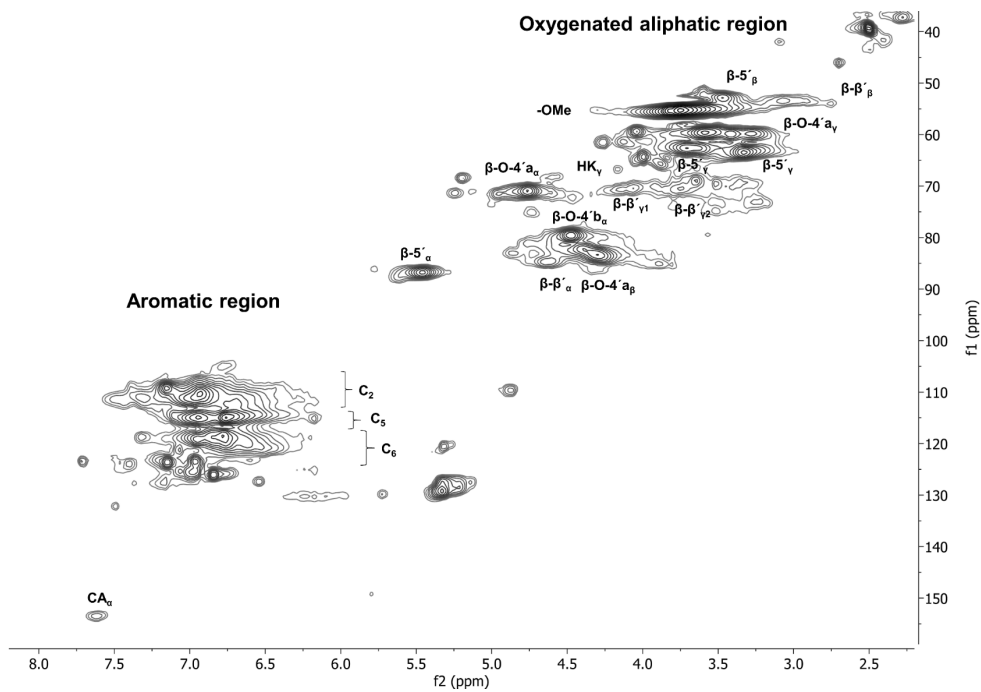


Figure S7. HSQC spectra of lignin sample D7. f1: ^{13}C , f2: ^1H .

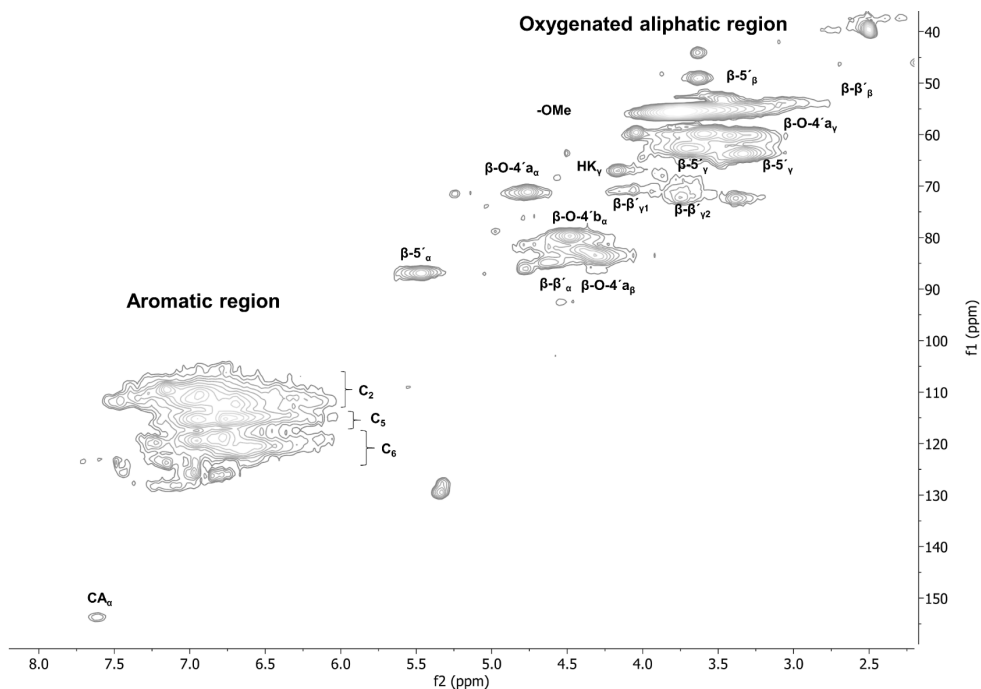


Figure S8. HSQC spectra of lignin sample D8. f1: ^{13}C , f2: ^1H .

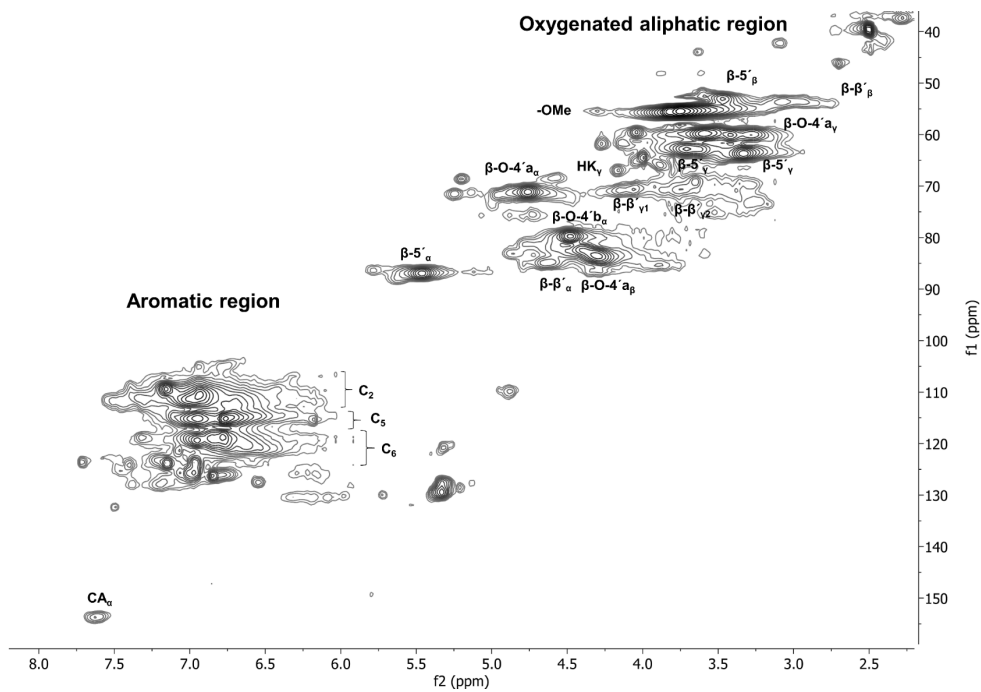


Figure S9. HSQC spectra of lignin sample D9. f1: ^{13}C , f2: ^1H .

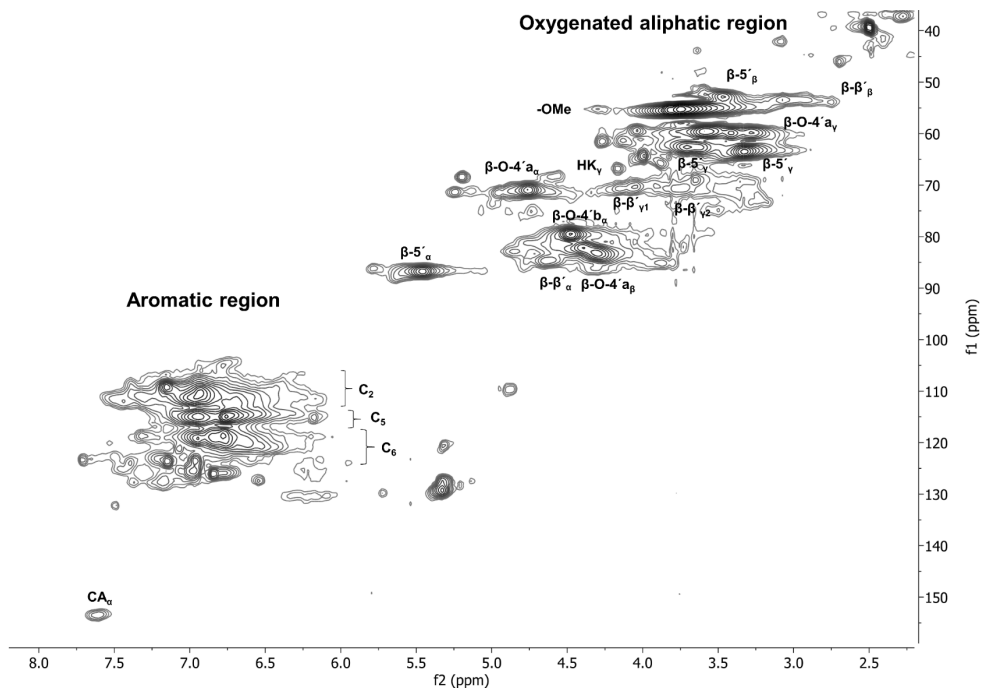


Figure S10. HSQC spectra of lignin sample D10. f1: ^{13}C , f2: ^1H .

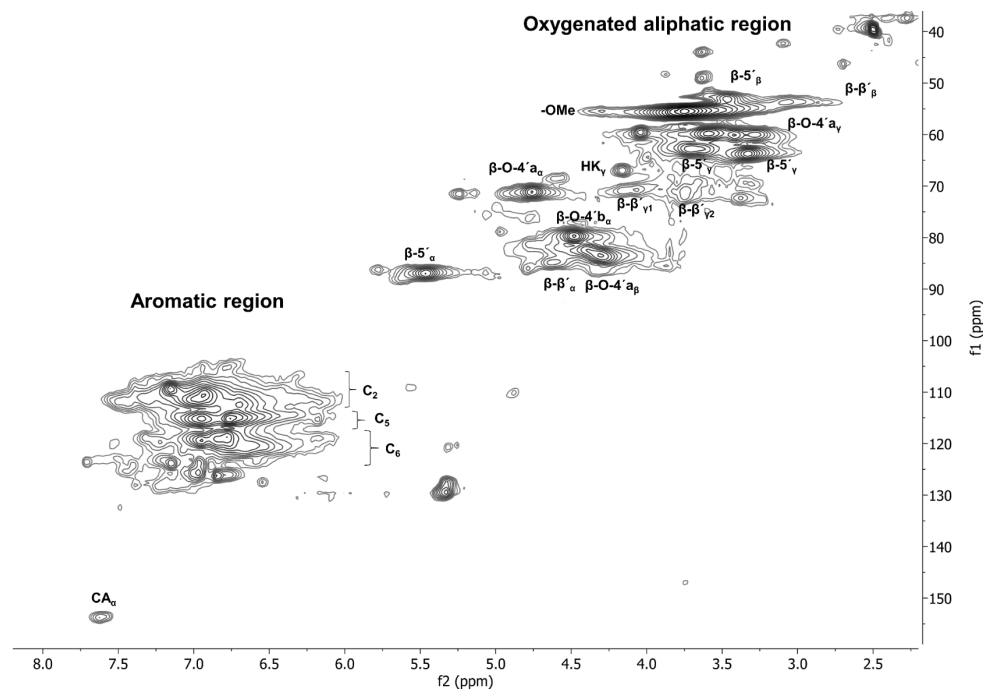


Figure S11. HSQC spectra of lignin sample D11. f1: ^{13}C , f2: ^1H .

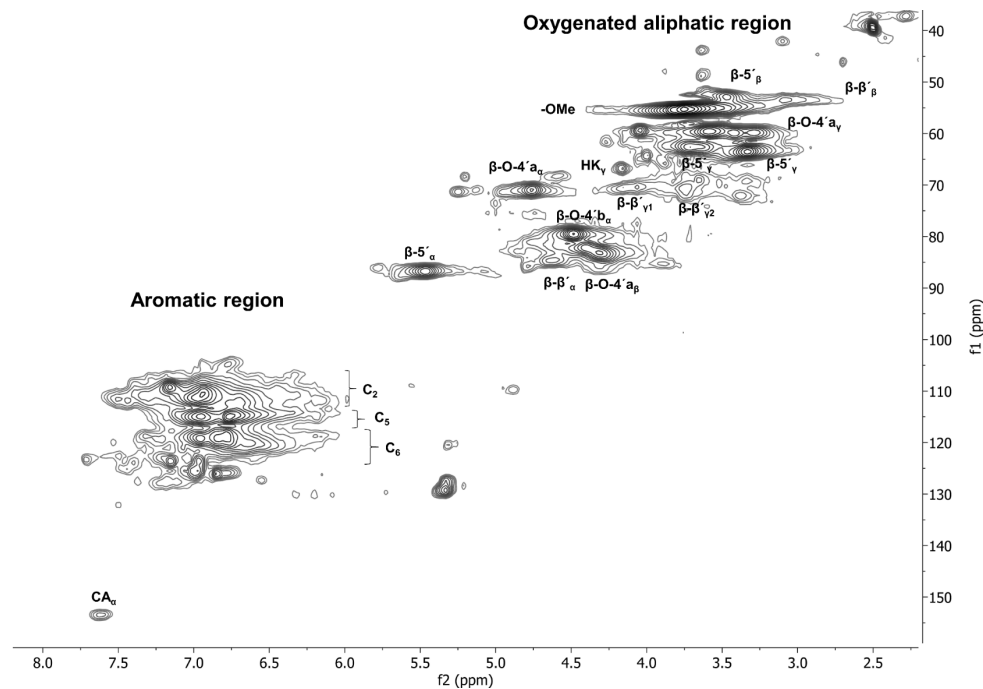


Figure S12. HSQC spectra of lignin sample D12. f1: ^{13}C , f2: ^1H .

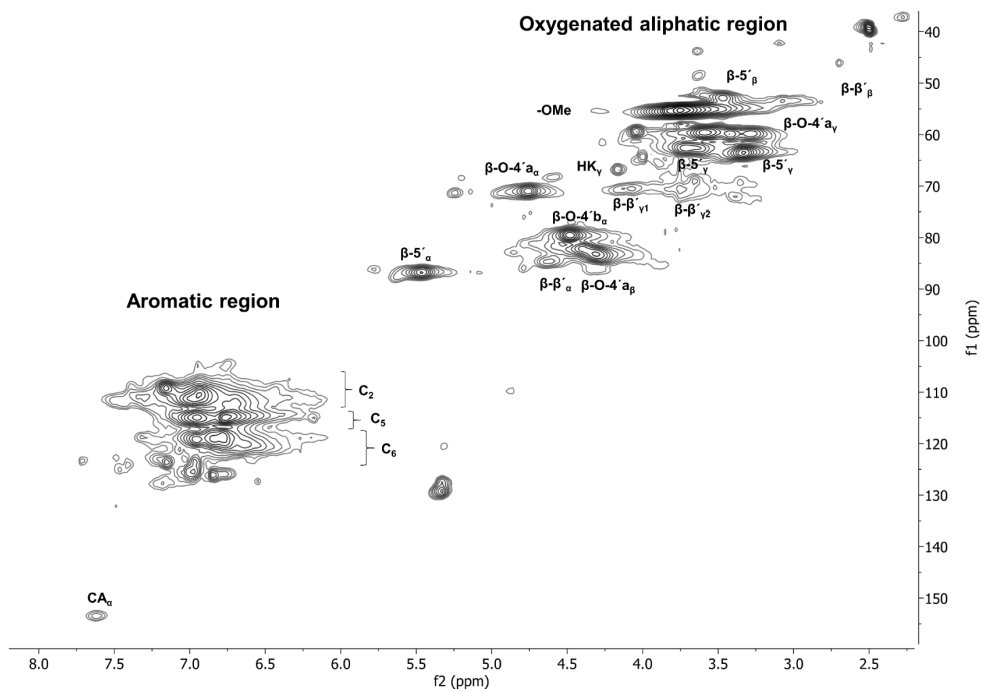


Figure S13. HSQC spectra of lignin sample D13. f1: ^{13}C , f2: ^1H .

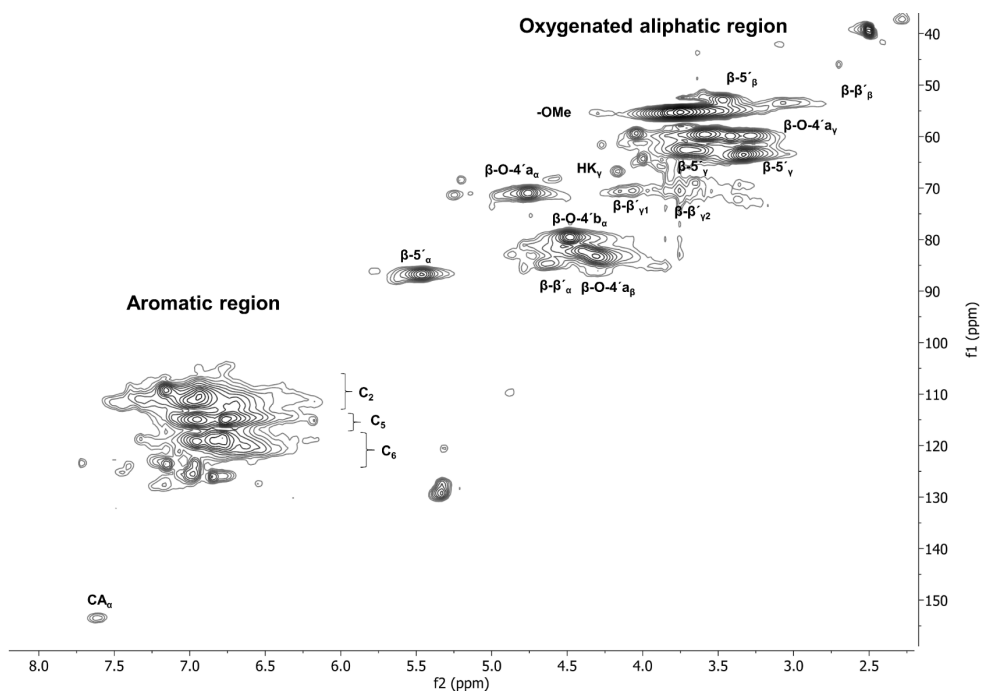


Figure S14. HSQC spectra of lignin sample D14. f1: ^{13}C , f2: ^1H .

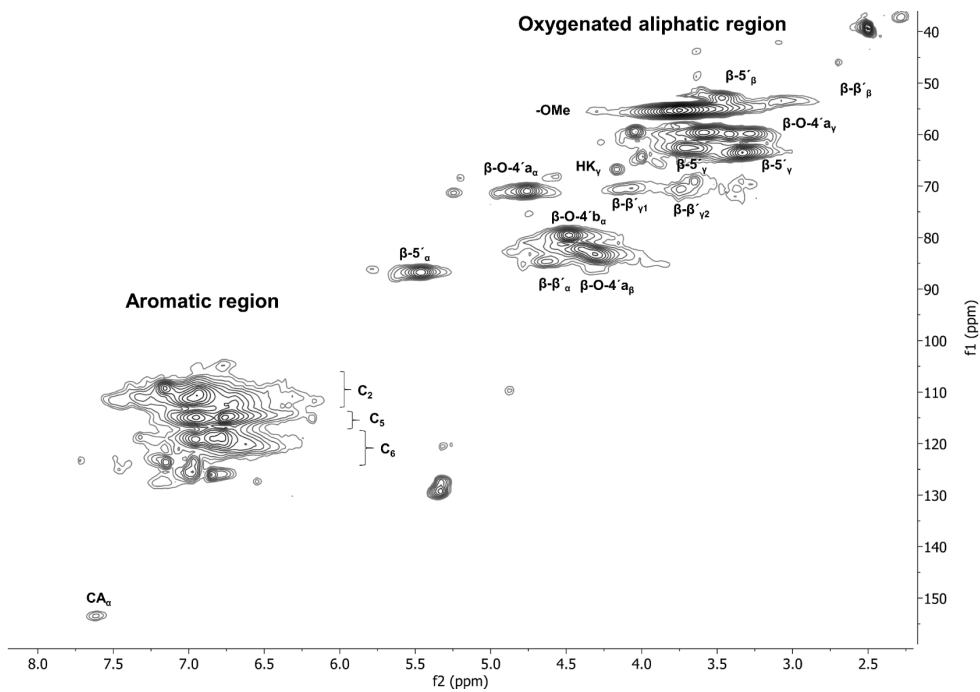


Figure S15. HSQC spectra of lignin sample D15. f1: ^{13}C , f2: ^1H .

1.5 Lignin spectra, Alcell and Kraft

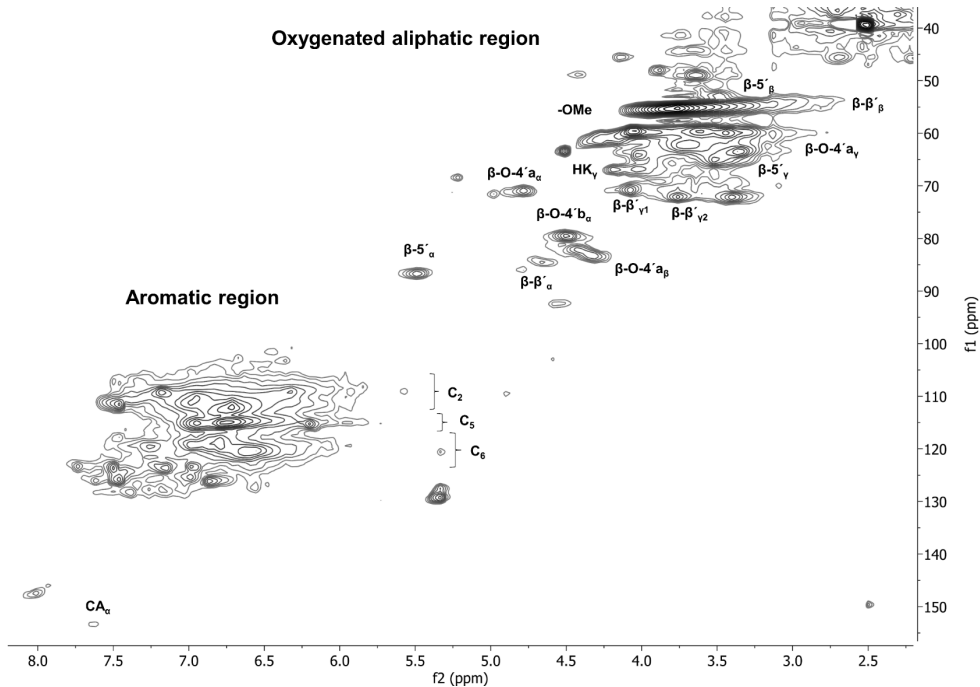


Figure S16. HSQC spectra of Alcell lignin. f1: ^{13}C , f2: ^1H .

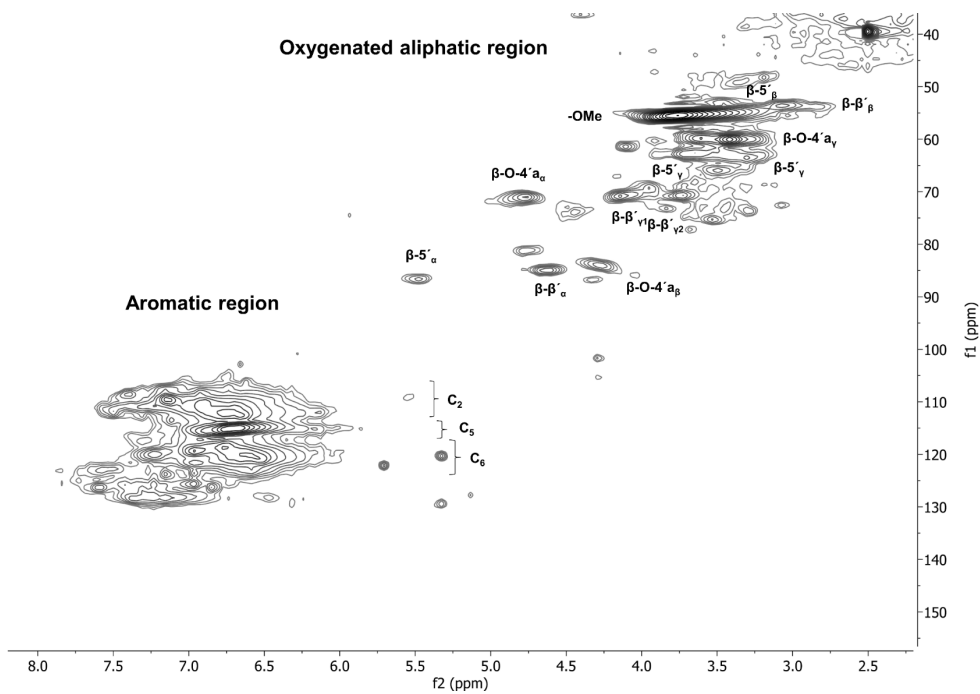


Figure S17. HSQC spectra of kraft lignin. f1: ^{13}C , f2: ^1H .

1.6 Water fraction from the cyclic organosolv extraction

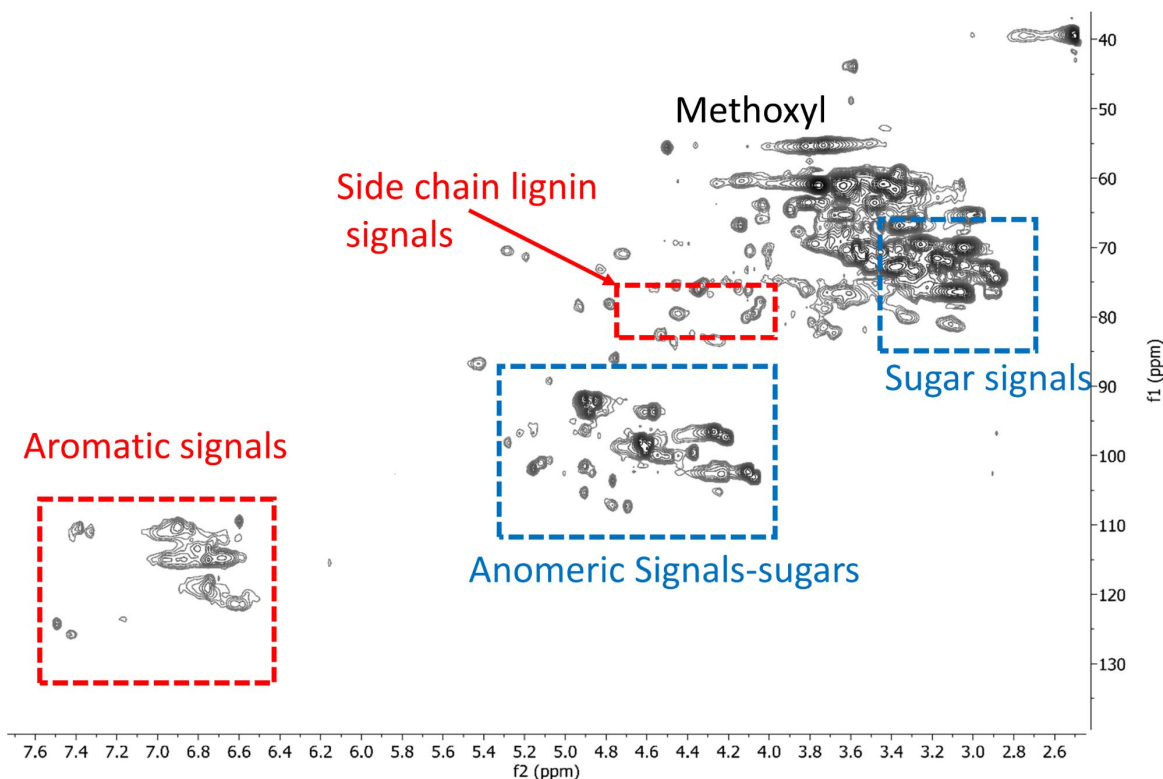


Figure S18. HSQC spectra of the water-soluble fraction of the cyclic organosolv lignin extraction. f1: ^{13}C , f2: ^1H .

1.7 Hemicellulose fraction from the hot water extraction

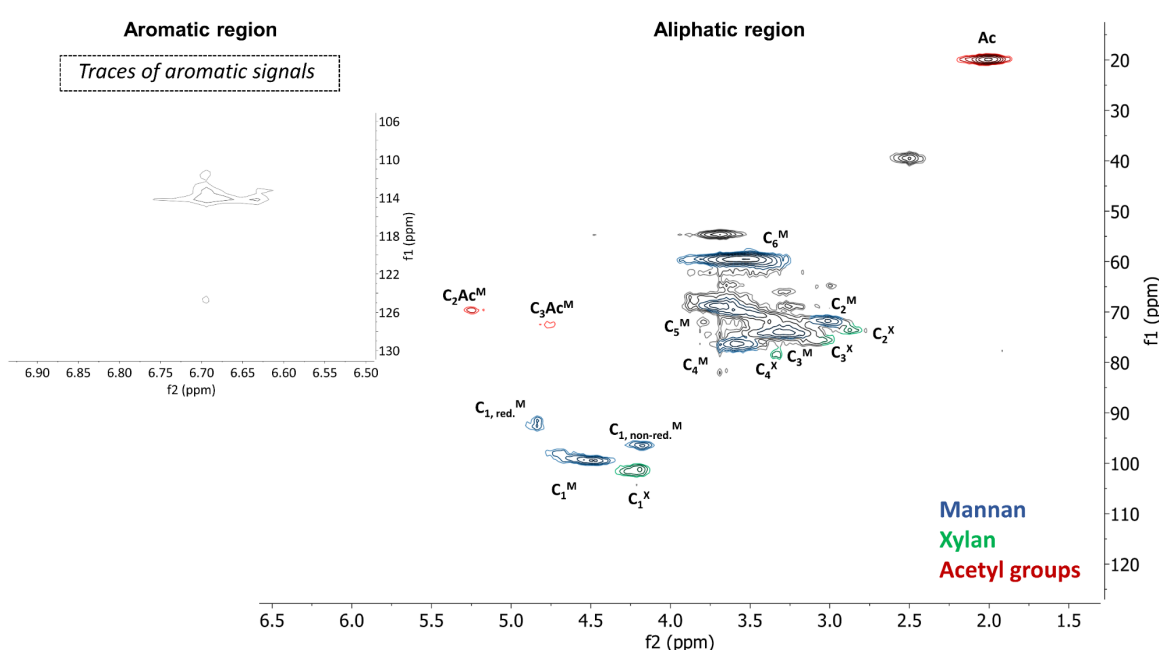


Figure S19. HSQC spectra of the hot water extracted fiber. f1: ^{13}C , f2: ^1H .

2. ^{31}P NMR

2.1 Assignment of chemical shifts, ^{31}P NMR

Table S4. The diagnostic chemical shifts are relative to the water reaction product of Cl-TMDP, at 132.2 ppm.

Hydroxyl functionality	ϵHNDI	Aliphatic-OH	Condensed-OH		Non-condensed-OH		Carboxylic acids-OH
			$\beta\text{5, 4-O-5, 5-5}$	Guaiacyl-OH	<i>p</i> -hydroxy phenyl-OH		
Chemical shift	152.3-151.7	149.1-145.1	144.7-141.1	140.6-138.8	138.2-137.3		136.6-133.6

2.2 Assigned phenolic hydroxyl-functionalities.

Table S5. Quantified hydroxyl functionalities, design serie.

Hydroxyl functionality	1	2	3	4	5	6	7	8	9	10	11	12	13-15 ¹
Aliphatic-OH	2.81	2.54	2.86	2.52	2.89	3.16	2.97	2.64	2.95	3.28	3.13	3.09	3.36 ± 0.10
Condensed-OH	0.39	0.88	0.33	0.88	0.36	0.62	0.37	0.90	0.39	0.37	0.62	0.60	0.54 ± 0.03
Guaiacyl-OH	1.27	1.56	1.33	1.58	1.39	1.26	1.29	1.58	1.14	1.18	1.44	1.30	1.29 ± 0.07
<i>p</i> -hydroxy phenyl-OH	0.07	0.07	0.04	0.08	0.06	0.06	0.06	0.06	0.05	0.05	0.05	0.06	0.06 ± 0.003
Carboxylic acids-OH	0.50	0.16	0.40	0.14	0.58	0.18	0.38	0.12	0.26	0.27	0.20	0.22	0.22 ± 0.01
Sum of aromatic-OH ²	1.73	2.51	1.70	2.54	1.81	1.93	1.72	2.54	1.58	1.60	2.11	1.97	1.88 ± 0.01

¹ n=3 ± SD

² the sum of aromatic-OH refers to the sum of the condensed-OH, guaiacyl -OH and the *p*-hydroxy phenyl-OH

Table S6. Quantified hydroxyl functionalities, Alcell benchmark.

Hydroxyl functionality	Aliphatic-OH	Condensed-OH	Guaiacyl-OH	<i>p</i> -hydroxy phenyl-OH	Carboxylic acids-OH	Sum of aromatic-OH ²
Alcell	1.36	1.16	1.49	0.18	0.33	2.83

2.3 Trends of aliphatic and aromatic hydroxyl functionalities

Stacked ^{31}P NMR spectra of samples D13, D4 and D3

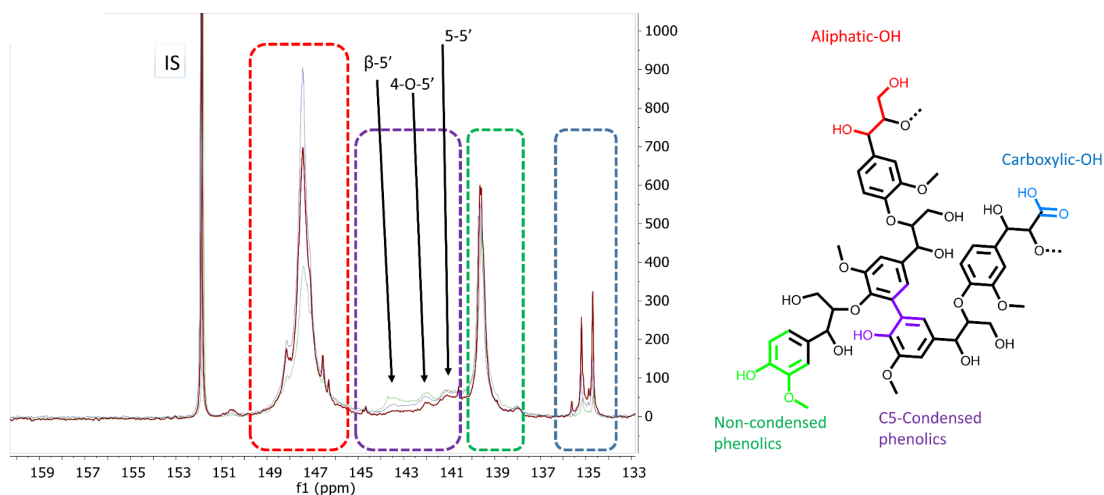


Figure S20. Stacked ^{31}P NMR spectra of sample D13, D4 and D3.

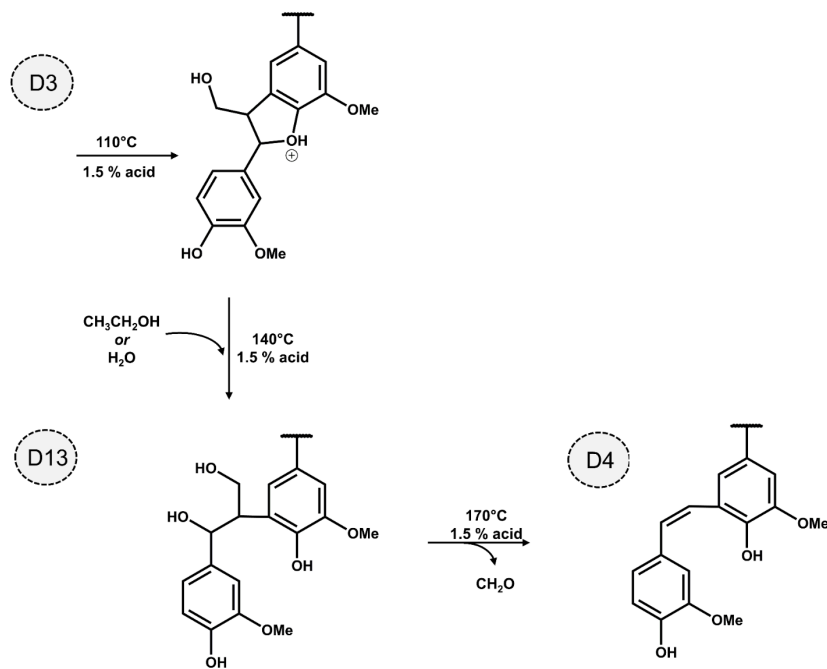


Figure S21. Mechanistic implications for different temperatures, illustrating the D13, D4 and D3 lignin samples.

3. ^{13}C NMR

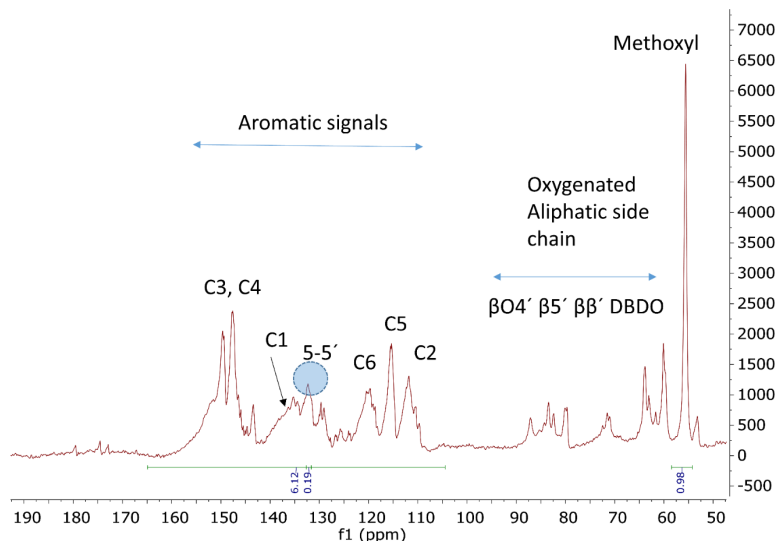


Figure S22. ^{13}C NMR spectra of the D12 sample. Quantification of 5-5' and DBDO substructures.

4. Size Exclusion Chromatography (SEC)

Table S7. THF-SEC, UV detection at 254 nm.

Design number	Temperature [°C]	EtOH [v%]	Acid [wt%]	Mn	Mw	D	DP _n
1	110	60	1.5	943	1952	2.07	5
2	170	60	1.5	1420	4401	3.10	8
3	110	80	1.5	991	2348	2.37	6
4	170	80	1.5	1508	7033	4.67	8
5	110	70	0.5	880	1918	2.18	5
6	170	70	0.5	1595	6771	4.24	9
7	110	70	2.5	1025	2418	2.36	6
8	170	70	2.5	1635	5949	3.64	9
9	140	60	0.5	1225	3150	2.57	7
10	140	80	0.5	1299	3695	2.84	7
11	140	60	2.5	1347	3555	2.64	7
12	140	80	2.5	1690	4827	2.86	9
13	140	70	1.5	1566	4557	2.91	9
14	140	70	1.5	1415	4082	2.88	8
15	140	70	1.5	1520	4126	2.72	8

Table S8. THF-SEC, UV detection at 254 nm.

Sample	Temperature [°C]	EtOH [v%]	Acid [wt%]	Mn	Mw	D	DP _n
Alcell	170	70	1.5	1380	13550	9.8	7

5. Differential Scanning Calorimetry (DSC)

Table S9. Investigation of glass transition temperatures (T_g) of a selection of samples.

Sample	Temperature [°C]	EtOH [v%]	Acid [wt%]	T_g^*
D3	110	80	1.5	181.8 ± 0.7
D4	170	80	1.5	182.4 ± 0.5
D6	170	70	0.5	177.5 ± 0.06
D7	110	70	2.5	184.3 ± 0.4
D13	140	70	1.5	151.3 ± 1
160	160	70	1.5	164.4 ± 0.2
Alcell	170	70	1.5	164.6 ± 0.5

* n=2, $\pm SD$

6. X-ray diffraction (XRD)

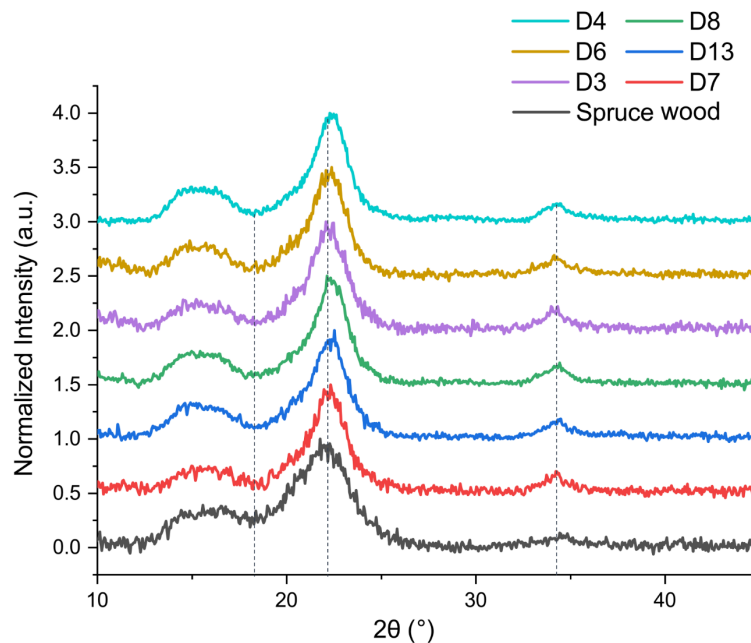


Figure S23. X-ray powder diffraction spectra of selected lignin fractions and native spruce wood, all samples were measured in duplicates.

7. Experimental design

7.1 Design matrix of the Box-Behnken design

Table S10. Design matrix using three center points; experiments 13-15.

Design number	Temperature [°C]	EtOH:H ₂ O [v/v]	Acid [wt%]
1	-1	-1	0
2	1	-1	0
3	-1	1	0
4	1	1	0
5	-1	0	-1
6	1	0	-1
7	-1	0	1
8	1	0	1
9	0	-1	-1
10	0	1	-1
11	0	-1	1
12	0	1	1
13	0	0	0
14	0	0	0
15	0	0	0

7.2 Tuning of the models

The models were tuned to improve the statistics for the experiments. Different transformation of the response data was needed, identified from skewness in the histogram for non-transformed data for some experiments, seen from the shape of the response distribution towards a normal distribution. The models were transformed as follows; Yield: logarithmic, aliphatic-OH: none, β-O-4': negative logarithmic, aromatic-OH: logarithmic, D: negative logarithmic, Mn: none.

7.3 Observed vs. predicted plot

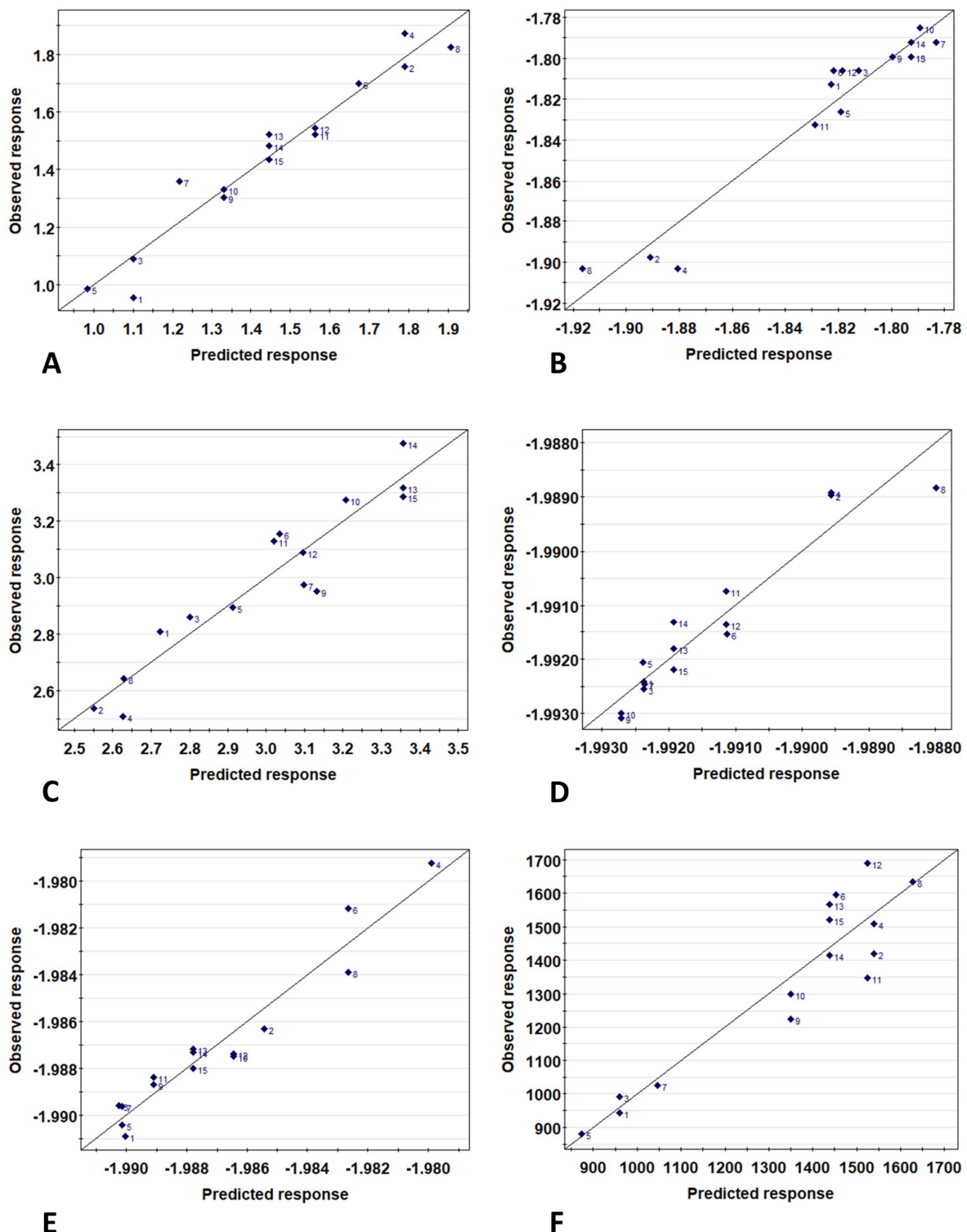


Figure S24. The plot illustrated the correlation between observed values vs. the predicted values from the model. The goodness of the model can be predicted in the observed vs. predicted plot. In a model with good predictions, the experimental points are close to the 1:1 line. The different responses follow this order; A: Yield, B: β -O-4', C: aliphatic-OH, D: aromatic-OH, E: D, F: Mn.

7.4 Normal probability plots

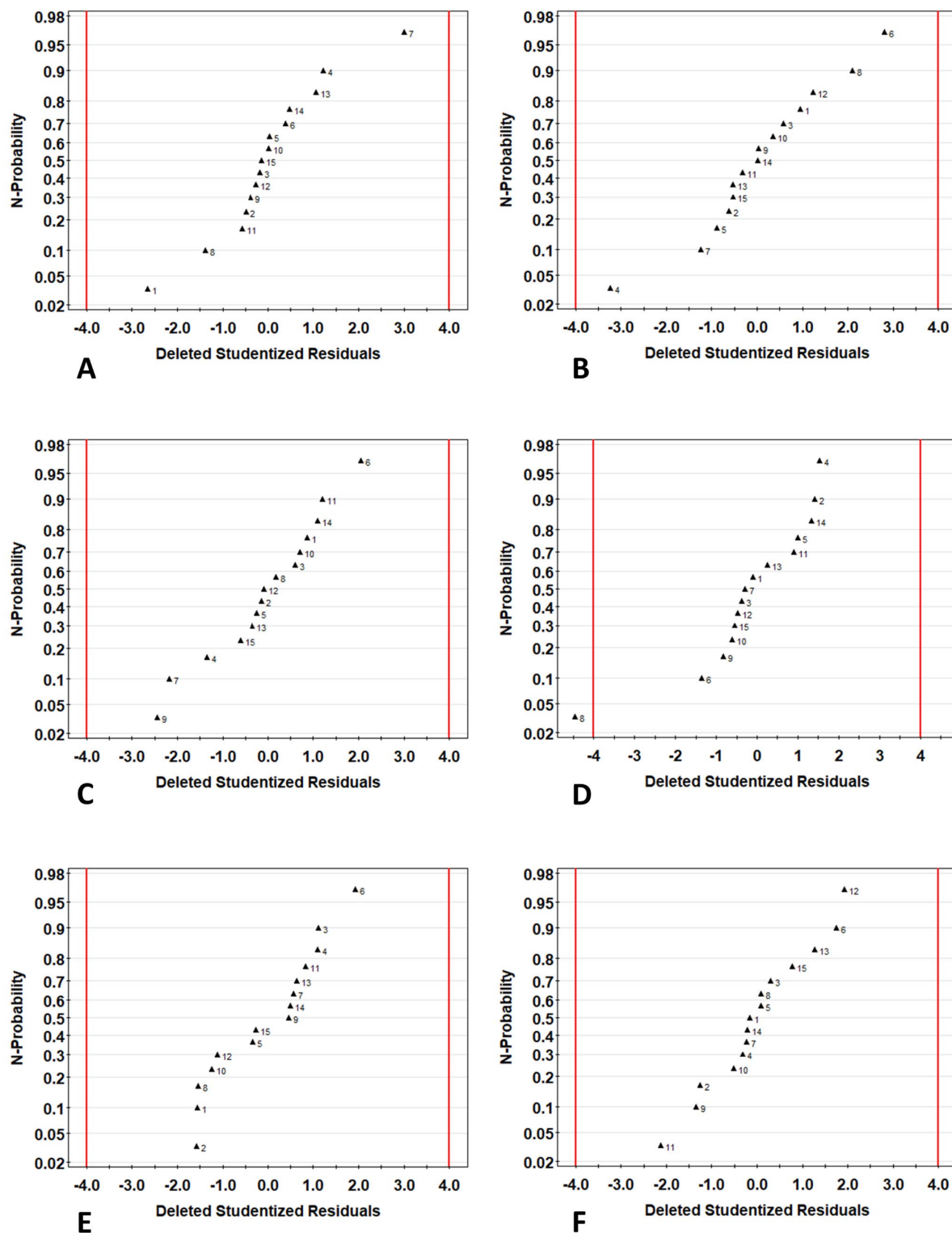


Figure S25. Investigation of the normal distribution of the error terms, and detection of potential outliers in the model. The experiments are indicated with the same numbers as in Table Sx. No outliers were detected within ± 4 standard deviation, except for aromatic-OH. An approximately linear plot illustrates approximately normal distributed error terms. A: Yield, B: $\beta\text{-O-}4'$, C: aliphatic-OH, D: aromatic-OH, E: D, F: Mn.

7.5 Normalized coefficient plot for Mn and D

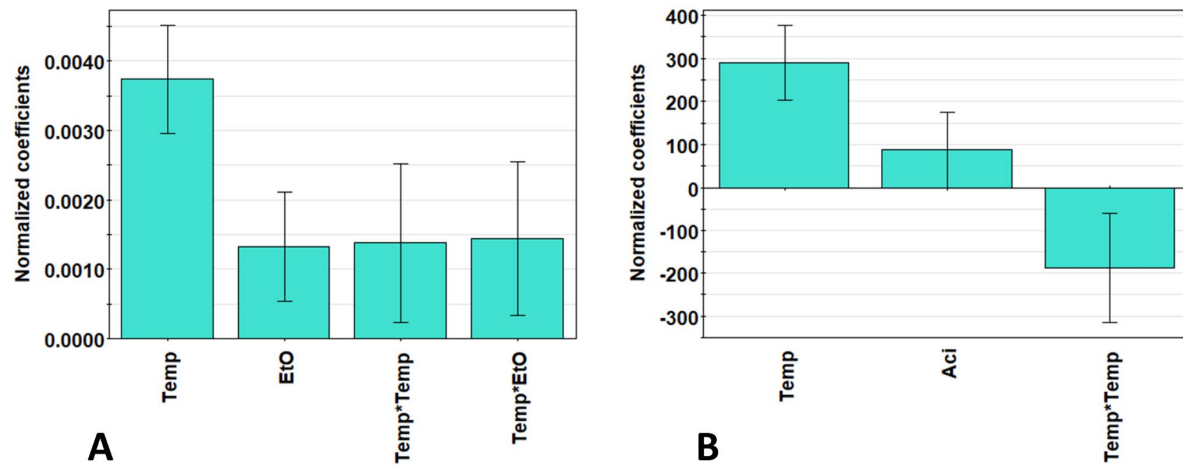


Figure S26. Normalized variables of dispersity, D, (A) and average molecular weight, Mn, (B) using 95% confidence level.

Table S11. All the optimized models shown significance and indications of good models in terms of a variance explained by the model (R^2), predictability of variation from cross-validation (Q_2), model validity and reproducibility.

Response	R2	Q2	Model validity	Reproducibility
Yield	0.94	0.90	0.65	0.98
β -O-4'	0.94	0.63	0.30	0.99
Aliphatic-OH	0.90	0.52	0.79	0.88
Aromatic-OH	0.91	0.67	0.81	0.94
D	0.93	0.80	0.54	0.98
Mn	0.86	0.74	0.73	0.92

7.6 Response surface plots

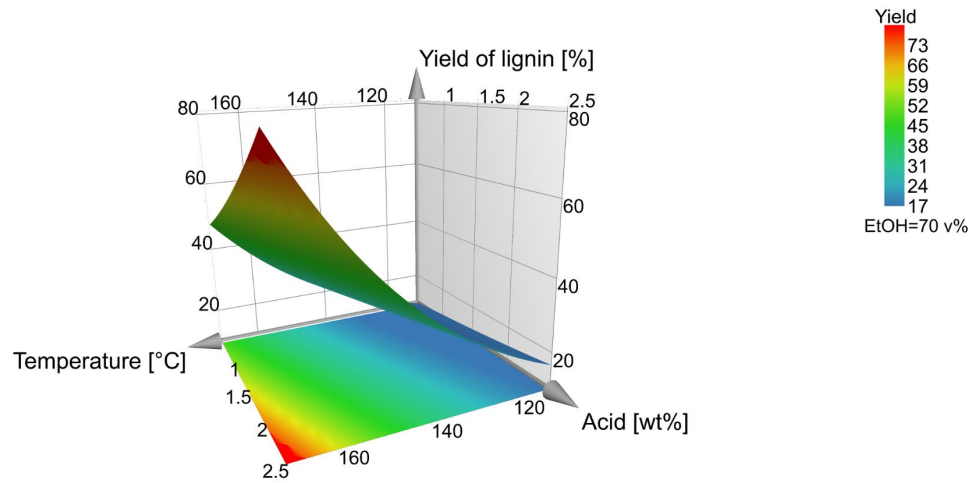


Figure S27. Yield. Since ethanol did not have significance in the model, its value is kept in the middle level.

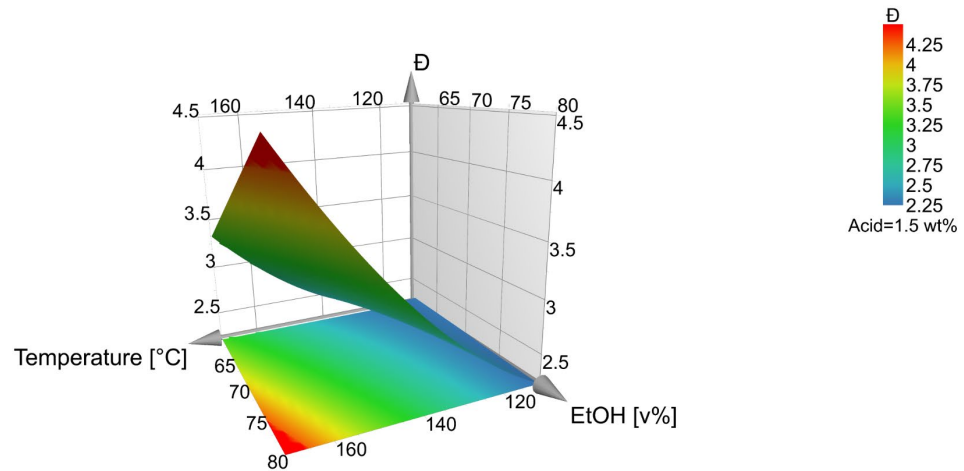


Figure S28. Molecular dispersity. Since the acid concentration was not significant for the model, its value is kept in the middle level in the illustration.

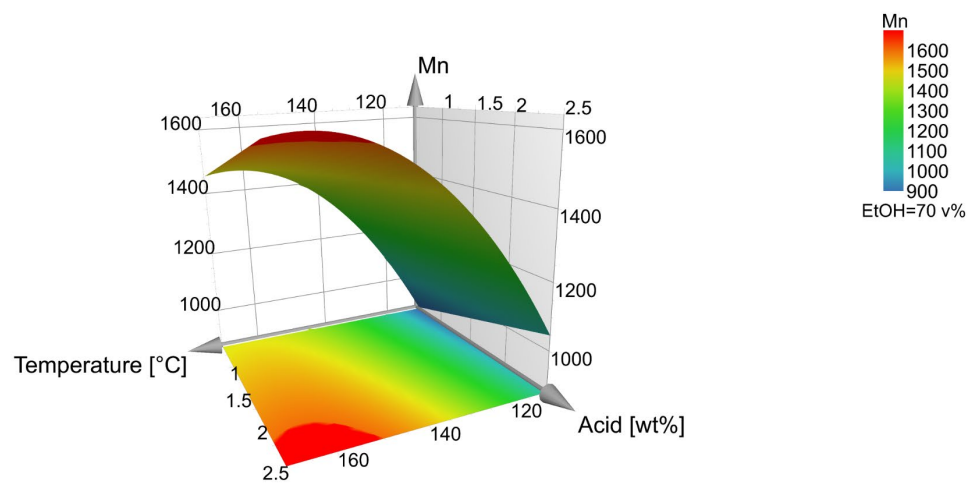


Figure S29. Mn. Since ethanol did not have significance in the model, its value is kept in the middle level.

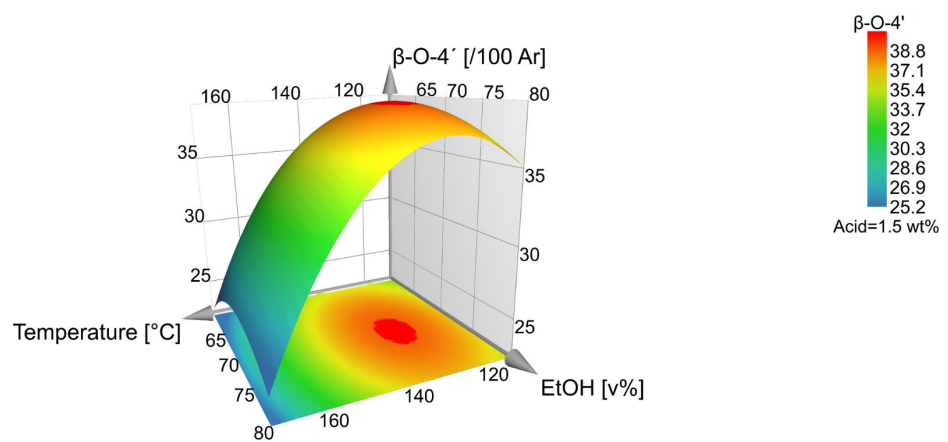


Figure S30. Ethanol influence on the $\beta\text{-O-}4'$ response. Acid concentration fixed at 1.5 wt% acid. The same effect on ethanol influence was shown for all levels of acid concentration and temperatures within the design, Table Xy. As illustrated in the graph, an overall shift of higher response and $\beta\text{-O-}4'$ content towards higher ethanol concentration, but with an optimum around 70 v%

8. Mass balance

The assigned yields of the fiber and lignin in Figure X and Table X are, in all cases, oven-dry weight-based.

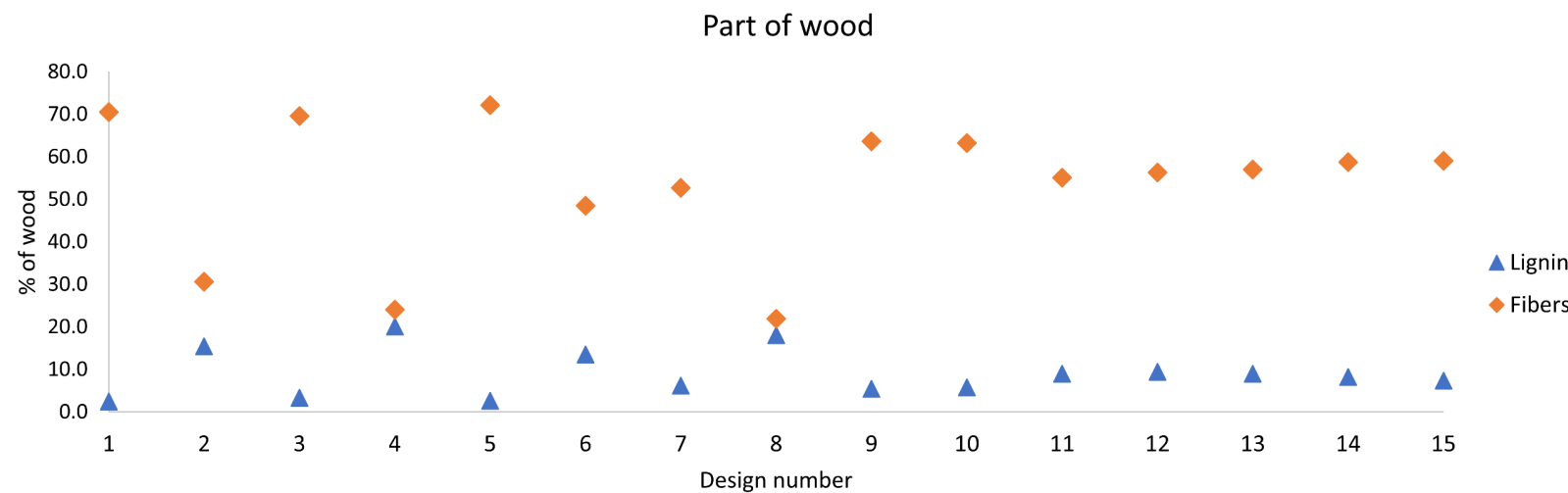


Figure S31. The mass % of the wood respectively the fiber.

Table S12. Extracted part of lignin in mass%, assuming 27% lignin in spruce wood. The hot water extraction, where the hemicellulose was extracted was same for all design experiments. The absolute mass of hemicellulose was 17.1 ± 0.99 , $n=3 \pm SD$. The Alcell experiment didn't include the hot water extraction and is therefore excluded.

Sample	Fiber residue ²	Part of lignin ²
D1	70.5	9.0
D2	30.7	57.3
D3	69.6	12.3
D4	24.1	74.5
D5	72.1	9.7
D6	48.5	50.1
D7	52.7	23.0
D8	21.9	67.0
D9	63.7	20.1
D10	63.2	21.4
D11	55.1	33.3
D12	56.3	35.1
D13	57.0	33.3
D14	58.8	30.4
D15	59.1	27.3
160	43.5 ± 0.8^3	52.3 ± 1.1^4
Alcell	N.A.	93.9

¹ Presented as % of the absolute mass

² Presented as the lignin in the starting material, assuming 27% lignin in spruce wood.

³ $n=2 \pm SD$ ⁴ $n=3 \pm SD$

9. Consolidated biorefinery concept

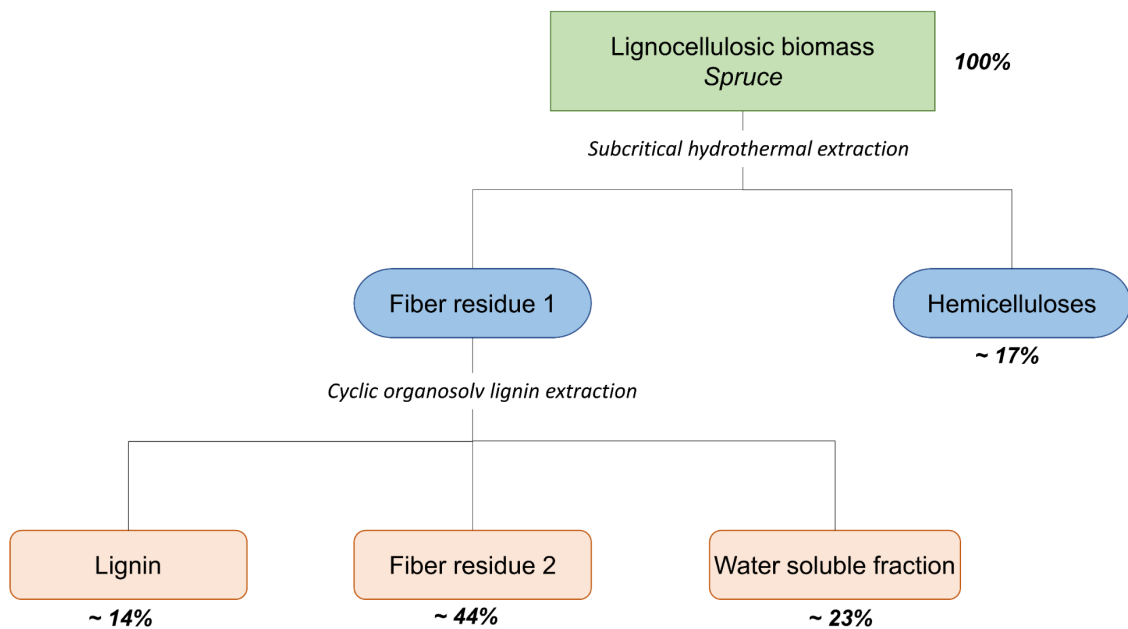


Figure S32. Schematic illustration of the previously developed consolidated biorefinery concept, with mass % of the different fractions. The process is divided into two major steps, wherein the first, the hemicellulose is extracted by subcritical water extraction, directly followed by the cyclic organosolv lignin extraction. For all experiments, the first step was using the same parameters, referring to water as an extraction solvent at a temperature of 160°C for 2h. The parameters for the cyclic organosolv lignin extraction were varied within this study. The mass % is based on a cyclic lignin extraction using 70:30 (v/v) EtOH: H₂O with 1.5 wt% H₂SO₄ as extraction solvent, at 160°C.

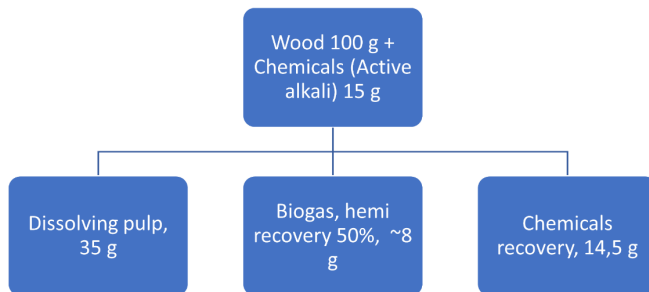
10. Carbohydrate analysis

Table S13. The monosaccharide composition and Klason lignin content of a selection of fiber residue 2 samples, presented as % of the absolute dry mass.

	Glucose	Xylose	Arabinose	Rhamnose	Mannose	Galactose	Total	Klason lignin
<i>% of absolute mass</i>								
Spruce 40 mesh	40.82	4.76	0.96	0.15	10.30	1.81	58.79	29.36
3	55.40	3.46	0.00	0.00	5.05	0.30	64.21	30.44
4	80.31	0.50	0.00	0.00	0.56	0.00	81.36	12.48
6	55.49	3.19	0.00	0.00	4.54	0.21	63.43	30.31
7	71.97	0.39	0.00	0.00	0.44	0.00	72.80	20.82
8	71.93	2.15	0.00	0.00	2.59	0.00	76.66	20.19
13	64.78	2.78	0.00	0.00	3.59	0.00	71.15	26.07

11. Green metrics

Kraft pulping



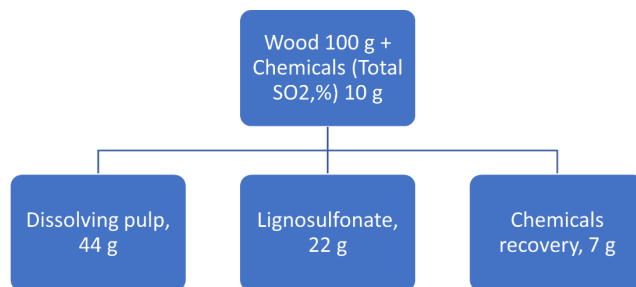
So the E-Factor will be;

$$= \frac{\text{Mass input } (100+15)-\text{Product output } (35+8+14.5)}{\text{Product output } (35 + 8+14.5)}$$

E-Factor = ~1

Figure S33. E-factor overview of the prehydrolysis kraft pulping. The E-factor is determined to be ~ 1.

Sulfite pulping



So the E-Factor will be:

$$= \frac{\text{Mass input } (100+10) - \text{Product output } (44+22+7)}{\text{Product output } (44+22+7)}$$

$$\text{E-Factor} = \sim 0.51$$

Figure S34. E-factor overview of the sulphite pulping. The E-factor is determined to be ~0.51.